Fluctuation modes of the frustrated XY-model

1991 J. Phys.: Condens. Matter 3 5955

(http://iopscience.iop.org/0953-8984/3/32/004)

J. Phys.: Condens. Matter 3 (1991) 5955–5966. Printed in the UK

Fluctuation modes of the frustrated XY-model

Keith A Benedict†‡§

† Department of Theoretical Physics, The Schuster Laboratory, The University, Manchester M13 9PL, UK

‡ Department of Physics, The Blackett Laboratory, Imperial College, London SW7 2BZ, UK

§ Department of Physics, The University, Nottingham, NG7 2RD, UK||

Received 17 December 1990, in final form 10 April 1991

Abstract. The spectrum of fluctuations around the flux density wave 'staircase' states of the frustrated XY-model of Josephson junction arrays is studied for rational values of the flux per plaquette, $f = p/q$. The structure of the Brillouin zone is discussed and the reduced eigenvalue equation for the Hessian matrix derived. The eigenvalue equation is studied analytically in two regions: (i) the zone boundary and (ii) the zone centre for the lowest band; in various limits as $q \to \infty$. Numerical diagonalization is employed for a sequence of values of f and the band structures and densities of states calculated. The simple harmonic approximation is modified to include the strong anisotropy of the states and is shown to explain the lowest band density of states well at low energy.

1. Introduction

The frustrated XY-model [1–3] has been widely used to describe the statistical mechanics of arrays of Josephson junctions and weak links such as artificial and natural granular superconductors and, most recently, sintered high temperature superconductors [4,5]. In this paper I will consider the excitations around a set of (meta)stable states of the model in two dimensions and in the absence of disorder, so the major experimental consequences are likely to be in the area of artificial arrays where the fluctuation spectra calculated here may well be observable via microwave absorption.

The rationality of the number of flux quanta, f, threading a unit cell of the array is a very important factor in the physics of these systems. For example, the graph of the network critical temperature versus f would be a very ramified, fractal line. Experimentally of course this ramification is only seen down to an energy scale set by the unavoidable disorder in the system. This dependence on the rationality of the flux is shared with the problem of the electronic states of a non-interacting gas of two-dimensional Bloch electrons in a strong magnetic field [6]. Halsey [7] constructed a set of states which extremize the Hamiltonian of the model and referred to them as 'staircase' states because of their structure. If one considers the self-consistent effect of the frozen-in supercurrents on the local magnetic field, then the state can be thought of as a flux density wave. The state is believed to be the ground state of the model for $1/3 < f < 2/3$ at least for q not too large. The flux density wave has, in addition to the obvious $U(1)$ degeneracy due to the invariance of the

|| Present address.

0953-8984/91/325955+12$03.50

Hamiltonian under global phase rotations, an additional $Z_2 \times Z_q$ degeneracy from the invariance under reflection in one of the lattice axes and from the invariance under translation by up to $q-1$ steps (translation by q steps maps the state onto inself). The fluctuations considered here will contribute to the low temperature properties of the system but there will be additional contributions from domain wall excitations between different, degenerate, states, as well as the excitation of vortex–antivortex pairs as in the conventional XY-model. The energetics of domain wall excitations will be the subject of a future paper. Much previous work on this subject has concentrated on the particularly simple case $f = 1/2$ [8–12]. A simple quasi-one-dimensional version [13, 14] has also been studied. The states can be constructed for any $f = p/q$ but the details of the spectra will depend strongly on p and q separately.

The fluctuations around the flux density wave will be described in terms of the eigenvalues of the Hessian, or stability matrix. The symmetries of the state allow the application of Bloch's theorem to the Hessian, leading to the labelling of the eigenvalues by a wavevector taking values in an anisotropic Brillouin zone and a q-valued band index. The reduced equation for the eigenvalues at fixed wavevector can be thought of as the tight-binding Schrödinger equation for a cyclic chain of q atoms with position dependent site energies and hopping elements. Analysis of the eigenvalues near the zone boundary is particularly simple and consists of simple quantum mechanical perturbation theory. Near the zone centre the behaviour of the lowest band can be analysed, particularly in the asymptotic limit $p, q \to \infty$: $p = p(q)$, by using the transfer matrix formalism [15]. This lowest band behaviour at the zone centre gives rise to an anisotropic harmonic approximation $\omega(\boldsymbol{k}) \sim \boldsymbol{k} \cdot \Gamma \cdot \boldsymbol{k}$, where Γ is the helicity modulus tensor, expected to be valid for low energies. Exact numerical diagonalization of the reduced Hessian leads to detailed pictures of the band-structure and density of states for particular values of $f = p/q$ which bear comparison with the analytic work. We shall be concerned with a sequence of values of f: $f_k = k/(2k+1)$ which, for $k > 1$ are in the regime in which the flux density wave is believed to be the ground state. The eigenvalue equation is a generalization of Harper's equation [16] and extension to weakly irrational values of f could be performed using the WKB method of Wilkinson [17].

The rest of this paper is arranged as follows. In section two the model will be described in detail, in section three the flux density wave state will be described, the Hessian matrix derived and its reduction via Bloch's theorem discussed. Section four contains the results of exact diagonalization of the reduced Hessian for representative values from the sequence f_k. Section five contains the analysis of the eigenvalues at the zone boundary, section six describes the behaviour of the lowest band at the zone centre and the harmonic approximation. Finally section seven contains a summary and discussion.

2. The frustrated XY-model

Consider a grain of superconducting material embedded in a normal matrix. Below the bulk transition of the superconductor (which will of course be strongly rounded out by finite size effects) there will be a non-zero value of the complex order parameter: $\psi = \rho e^{i\theta}$. Thermal fluctuations in the amplitude, ρ, will be resisted by an effective restoring force (in the language of field theory they are massive), while fluctuations in the phase angle, θ, corresponding to the Goldstone mode of the bulk

transition, will be completely free. Now consider a regular array of such grains with large intergrain separations. The amplitudes on each grain will be approximately the same but the phases, θ_i, will fluctuate in time and vary randomly from one grain to another. If the spacing of the grains is now made very much smaller, then tunnelling between different grains becomes possible; the effect of tunnelling (either the Josephson effect if the matrix is an insulator or the proximity effect if the matrix is a normal metal) is to favour phase coherence between grains. From the theory of Josephson junctions we can write down an effective free energy for the phase fluctuations of the form

$$H = -J(T) \sum_{(i,j)} \cos(\theta_i - \theta_j). \tag{2.1}$$

This is the Hamiltonian for the normal *XY*-model (albeit with a temperature-dependent coupling constant). Consequently we can expect the system to have an additional phase transition at which the network orders (either long range ordering of the phases if the space dimensionality is three or algebraic order in two dimensions). Such effects have been observed both in artificial granular materials and wire arrays and in samples of sintered $YBa_2Cu_3O_7$. If an external magnetic field h is applied to the array then the form of this free energy is modified by the replacement of the phase difference by the gauge-invariant quantity $\phi_{i,j} = \theta_i - \theta_j - A_{i,j}$, where the twist, A, is defined as

$$A_{i,j} = \frac{2\pi}{\Phi_0} \int_i^j \boldsymbol{A}(\boldsymbol{r}) \cdot \mathrm{d}\boldsymbol{l}. \tag{2.2}$$

Φ_0 is the appropriate flux quantum and the vector potential satisfies

$$\nabla \times \boldsymbol{A} = \boldsymbol{B} = \boldsymbol{h} - g\boldsymbol{M} \tag{2.3}$$

where $\boldsymbol{B}$ is the local magnetic field and $\boldsymbol{M}$ is the circulation of current around the plaquette which is proportional to the local magnetization. It is conventional to neglect the self-consistent aspect of this problem, i.e. to set $g = 0$. Preliminary numerical evidence suggests that this is not a serious omission if one is looking at ground state properties of the array (indeed in real arrays of ~ 5 μm diameter with $f = 1/2$ it has the numerical value $g \sim 10^{-3}$ [16]), but it seems quite likely that this may be very misleading in the study of, for example, the network critical current. Since we will be dealing entirely with small fluctuations around the ground state we will also make this approximation.

From now on we will restrict attention to a system consisting of a two-dimensional square lattice of grains. It is straightforward to see that the sum of the twists around an elementary plaquette, α, of the lattice is given by

$$\sum_{(i,j)\in\partial\alpha} A_{i,j} = 2\pi f_\alpha \tag{2.4}$$

where $f_\alpha = \Phi_\alpha/\Phi_0$ is the flux through the plaquette in units of the flux qauntum. It is also the case that f is a measure of the frustration on a plaquette. If f is an integer then the twist around the plaquette adds up to a whole number of complete rotations and can be gauged away: the energy associated with each bond of the lattice

can be minimized simultaneously; if f is not an integer then this cannot be done and the plaquette is frustrated.

The current flowing across a junction is given by the expression

$$I_{i,j} = \frac{2e}{\hbar} J(T) \sin(\phi_{i,j}) \tag{2.5}$$

and we therefore identify $2eJ(T)/\hbar$ with the critical current of the single bond. If f is not an integer then no configuration exists in which all the phase differences are zero and therefore any state, including the ground state, has currents flowing.

The condition that a phase configuration $\overline{\theta_i}$ be an extremum of the Hamiltonian H is that

$$\left(\frac{\partial H}{\partial \theta_i}\right)_{\overline{\theta_i}} = \sum_{j:|i-j|=1} J(T) \sin(\phi_{i,j}) = 0 \tag{2.6}$$

that is, Kirchoff's law is satisfied at each node of the network. In all of the following we shall be considering the system at zero temperature and so the coupling constant will be $J = J(0)$.

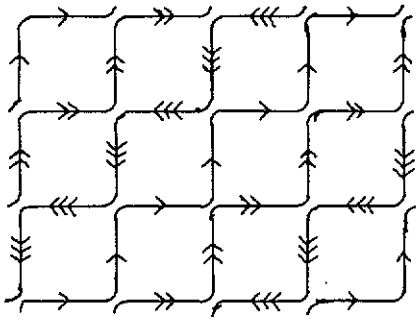

Figure 1. The staircase structure showing the assignment of bonds to a unique staircase and the current flows in the flux density wave state.

3. The flux density wave state

Halsey [7] constructs the flux density wave state explicitly in terms of the phase angles, θ_i, here we only require the values of the gauge-invariant phase differences, $\phi_{i,j}$. The construction is based on the assignment of each bond of the lattice to a unique staircase (see figure 1). The state is constructed such that the current is the same on each bond of a given staircase, which automatically fulfills equation (2.6). We shall refer to a lattice site by its coordinates x, y and define the phase differences

$$\phi^x_{x,y} = \phi_{x,y;x-1,y} \qquad \phi^y_{x,y} = \phi_{x,y;x,y-1}. \tag{3.1}$$

The staircase form entails the relations

$$\sin(\phi^x_{x,y}) = \sin(\phi^x_{x-y,0}) \qquad \sin(\phi^y_{x,y}) = \sin(\phi^x_{x-y+1,0}) \tag{3.2}$$

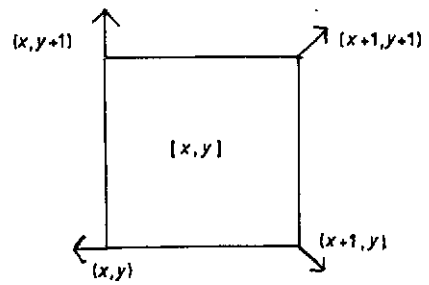

Figure 2. An elementary plaquette of the lattice labelled $[x, y]$.

in order that the state constructed be a minimum we shall require that the phase differences all lie in the interval $-\pi/2 < \phi < \pi/2$ and so we can set

$$\phi^x_{x,y} = \varphi_{x-y} \qquad \phi^y_{x,y} = \varphi_{x-y+1} \tag{3.3}$$

Consider the plaquette shown in figure 2; the sum of the gauge invariant phase differences around the plaquette must equal the sum of the twist factors (the θs cancel pairwise) and so

$$2(\varphi_{x-y+1} - \varphi_{x-y}) = 2\pi f \tag{3.4}$$

or

$$\varphi_z = \varphi_0 + z\pi f + k\pi \tag{3.5}$$

where k is an integer chosen to bring φ into the correct interval. The energy of the state is then minimized with respect to the phase, φ_0, yielding the result (cf [7] for details)

$$\varphi_0 = \begin{cases} \pi/2q & q \text{ even} \\ 0 & q \text{ odd.} \end{cases} \tag{3.6}$$

For example, in the case $f = 1/3$ the phase differences are: $\varphi_0 = 0$, $\varphi_1 = \pi/3$ and $\varphi_2 = -\pi/3$; while in the case $f = 2/5$ they are $\varphi_0 = 0$, $\varphi_1 = 2\pi/5$, $\varphi_2 = -\pi/5$, $\varphi_3 = \pi/5$ and $\varphi_4 = -2\pi/5$. Equivalent but distinct states can be formed by (i) global rotation of all the phase angles, (ii) reflection in the y-axis and (iii) translation by $1, 2 \ldots q-1$ lattice spacings in the y-direction. Hence the state has a $U(1) \times Z_2 \times Z_q$ degeneracy (for $q > 2$). The energy per grain of the flux density wave state of a system of size $L \times L$ is given by

$$\begin{aligned} E &= -\frac{J}{L^2}\sum_{x=1}^{L}\sum_{y=1}^{L}\{\cos(\phi^x_{x,y}) + \cos(\phi^y_{x,y})\} = -\frac{2J}{q}\sum_{i=1}^{q} A_i \\ &= -2JL_+(q)/q \end{aligned} \tag{3.7}$$

where $A_z = \cos(\varphi_z)$ and L_+ is defined as the sum of the q A_is.

The magnetization produced by the supercurrents in the plaquette (x, y) of figure 2 is given by

$$\begin{aligned} M_{x,y} &= \frac{2e}{\hbar}J[\sin(\phi^x_{x+1,y}) + \sin(\phi^y_{x+1,y+1}) - \sin(\phi^x_{x+1,y+1}) - \sin(\phi^y_{x,y+1})] \\ &= \frac{4e}{\hbar}J[\sin(\varphi_{x-y+1}) - \sin(\varphi_{x-y})] = m_{x-y} \end{aligned} \tag{3.8}$$

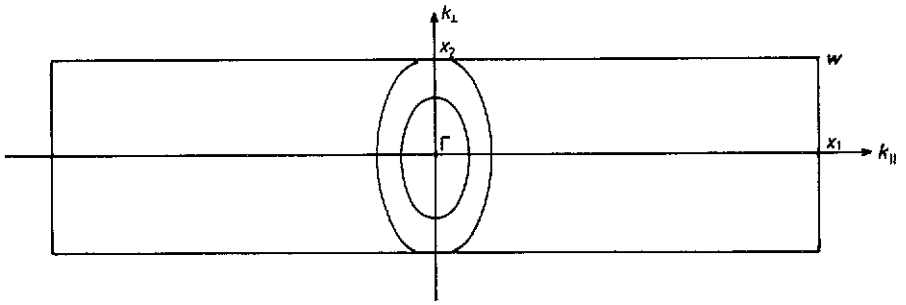

Figure 3. The shape of the Brillouin zone for fluctuations around the $f = p/q$ flux density wave state showing two constant (low) energy curves.

the flux density is therefore modulated perpendicular to the staircase as

$$\Phi_{x-y} = f\Phi_0 - gm_{x-y} + O(g^2) \tag{3.9}$$

where Φ_0 is the flux quantum. It is straightforward to find the Hessian matrix:

$$\begin{aligned} M_{x',y';x,y} &= \left(\frac{\partial^2 H}{\partial\theta_{x',y'}\partial\theta_{x,y}}\right)_{f\,\mathrm{d}w} \\ &= J\{A_{x+y}(2\delta_{x',x}\delta_{y',y} - \delta_{x'+1,x}\delta_{y',y} - \delta_{x',x}\delta_{y'+1,y}) \\ &\quad + A_{x+y+1}(2\delta_{x',x}\delta_{y',y} - \delta_{x'-1,x}\delta_{y',y} - \delta_{x',x}\delta_{y'-1,y})\}. \end{aligned} \tag{3.10}$$

The eigenvalue equation for the Hessian has the form

$$M_{x,y;x',y'}v_{x',y'} = \omega v_{x,y}$$

or

$$A_{x+y}\{2v_{x,y} - v_{x-1,y} - v_{x,y-1}\} + A_{x+y+1}\{2v_{x,y} - v_{x+1,y} - v_{x,y+1}\} = \frac{\omega}{J}v_{x,y}. \tag{3.11}$$

The periodicity of the Hessian allows the use of Bloch's theorem to express the eigenfunctions in the form

$$v_{x,y} = \mathrm{e}^{\mathrm{i}k_\parallel(x-y)}\mathrm{e}^{\mathrm{i}k_\perp(x+y)}C^{(k)}_{x+y} \tag{3.12}$$

where the wavevector k takes values in the anisotropic Brillouin zone shown in figure 3. with

$$k_\parallel \in [-\pi/2, \pi/2] \qquad k_\perp \in [-\pi/2q, \pi/2q] \tag{3.13}$$

and the Bloch function C has period q and satisfies the reduced equation

$$(A_i + A_{i+1})C^{(\nu)}_i - xz^* A_i C^{(\nu)}_{i-1} - xzA_{i+1}C^{(\nu)}_{i+1} = \tfrac{1}{2}\Lambda^{(\nu)}(x,z)C^{(\nu)}_i \tag{3.14}$$

where $x = \cos(k_\parallel)$, $z = \mathrm{e}^{\mathrm{i}k_\perp}$ and ν is a q-valued band index. The energy $\omega(k_\parallel, k_\perp) = J\Lambda(\cos(k_\parallel), \cos(k_\perp))$ is then a q-branched function defined on the Brillouin zone of figure 3.

The case $f = 1/2$ is easily solvable for all points in the Brillouin zone. The phase differences are $\varphi_0 = \pi/4$ and $\varphi_1 = -\pi/4$ hence $A_x = 1/\sqrt{2} \quad \forall x$. The Bloch equation has the form

$$\det\begin{bmatrix} 1-(\Lambda/2\sqrt{2}) & -x\eta \\ -x\eta & 1-(\Lambda/2\sqrt{2}) \end{bmatrix} = 0$$

where $\eta = \cos(k_\perp) = \frac{1}{2}(z + z^*)$. Hence

$$\tfrac{1}{8}\Lambda^2 - \tfrac{1}{\sqrt{2}}\Lambda + (1 - x^2\eta^2) = 0$$

which has solutions

$$\omega(k_\parallel, k_\perp) = 2\sqrt{2}J(1 \pm \cos(k_\parallel)\cos(k_\perp)).$$

On quite general grounds we know that, near the zone centre, the lowest band will correspond to the Goldstone modes of the network ordering transition and the eigenvalue $\omega^{(0)}(0,0)$ will be zero since it corresponds to global rotations of the phase angles.

4. Exact diagonalization for finite q

The reduced Hessian is a $q \times q$ Hermitian matrix which can be diagonalized using standard numerical methods. This has been done for a number of values of f from the sequence $f_k = k/(2k+1)$. Some of the results are shown in figures 4 to 8.

Figure 4 shows sections of the dispersion $\omega(k)$ along three lines in the Brillouin zone for $f = 3/7$. The left hand graph of figure 5 is a close-up of the region near the $X_\parallel$ point along the $k_\perp = 0$ line. Notable features of these band structures include the fact that at $k_\parallel = \pi/2$ ω is independent of $k_\perp$, that $\omega(k)$ is relatively flatter in the $k_\perp$ direction than in the $k_\parallel$ direction at the zone centre, and that the middle band is exceedingly flat.

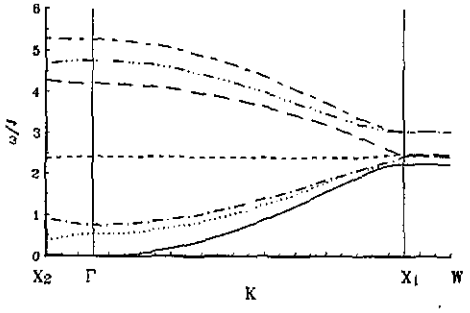

Figure 4. Sections of the energy surfaces along three lines of the Brillouin zone for the case $f = 3/7$.

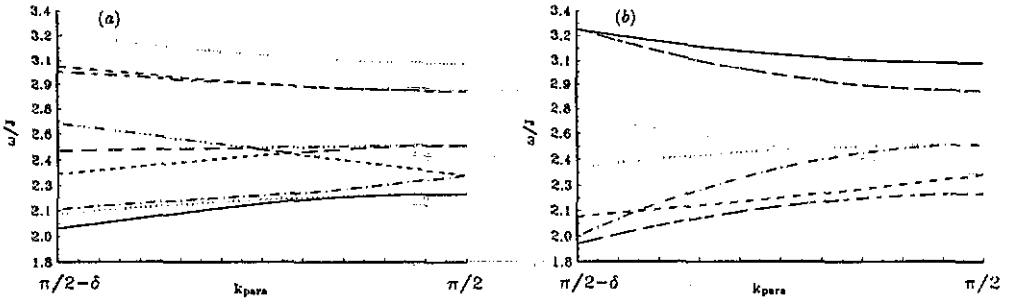

Figure 5. The variation of the eigenvalues close to the zone boundary. (*a*) exact numerical result, (*b*) given by second order perturbation theory for $f = 4/9$, $\delta = \pi/20$.

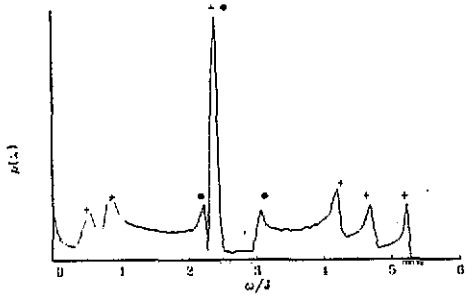

Figure 6. The density of states of the Hessian matrix for $f = 3/7$, ● indicates the positions of the energy levels at the $X_{\|}$, + the energy levels at Γ.

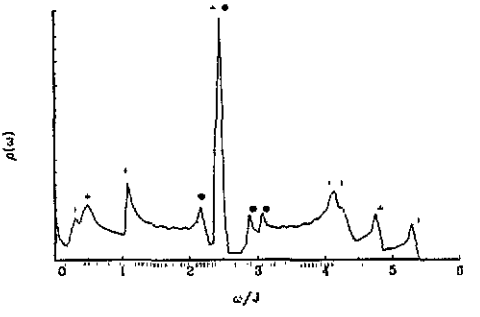

Figure 7. The density of states of the Hessian matrix for $f = 4/9$, ● indicates the positions of the energy levels at the $X_{\|}$, + the energy levels at Γ.

Figures 6 and 7 show the density of states of the Hessian for the cases $f = 3/7$ and $f = 4/9$ respectively while figure 8 shows a close up of the low energy ($0 < \omega < 0.1J$) density of states for the case $f = 4/9$. The most striking features of the graphs 6 and 7 are the abundance of peaks in the spectrum, including one very pronounced peak close to the centre of the energy range. At low energy two regimes are obvious: at the very lowest energy the density of states is a constant, as one might exepect for a two-dimensional system, but above some value of ω it drops off in a way that one normally associates with a one-dimensional system $\rho(\omega) \sim \omega^{-1/2}$.

The complete flatness of the bands at the short zone boundary clearly is the cause of the peaks in the density of states in the middle of the energy range while the extreme flatness of the middle band at all points in the zone is responsible for the very large central peak. The remaining sections of the paper will discuss the flatness at the zone boundary and the reason for the 2D/1D crossover which will be seen to be responsible for the peaks in the density of states at the extremes of the energy range.

5. Behaviour at the zone boundary

The reduced eigenvalue equation (3.14) can be thought of as the tight-binding Schrödinger equation for a particle on a cyclic chain of q sites with one localized state per site corresponding to the Hamiltonian $H = H_0 + xV$ where

$$H_0 = \sum_{i=1}^{q} (A_i + A_{i+1})|i\rangle\langle i|$$
$$V = -\sum_{i=1}^{q} \{z^* A_i |i\rangle\langle i-1| + z A_{i+1} |i\rangle\langle i+1|\} \tag{5.1}$$

where $x = \cos(k_\parallel)$ and $z = e^{ik_\perp}$. The Schrödinger equation then has the form $\langle i|H|\psi\rangle = \frac{1}{2}\Lambda\langle i|\psi\rangle$ where $\Lambda = \omega/J$. At the 'short' zone boundary $k_\parallel = \pi/2$ so $x = 0$ and the Hamiltonian (4.1) is diagonal with eigenstates

$$H_0|i\rangle = (A_i + A_{i+1})|i\rangle. \tag{5.2}$$

For $f = k/(2k+1)$ the A_is are given by

$$A_{2i+1} = \cos\left(\frac{k-i}{2k+1}\pi\right) \qquad A_{2i} = \cos\left(\frac{i}{2k+1}\pi\right) \tag{5.3}$$

which satisfy the relation $A_i = A_{2k+1-i}$. The state $|k\rangle$ is non-degenerate in both cases and has energy $\lambda^0(0) = 4A_k$, while all the other states are two-fold degenerate with states $|k+i\rangle$ and $|k-i\rangle$ having energies $\lambda^i(0) = 2(A_{k+i} + A_{k+i+1})$. The ordering of the energy levels depends on both p and q, for $p = 1$, $q = 2k+1$ the singlet $|k\rangle$ is the lowest level and the doublet $|k \pm i\rangle$ is the ith pair from the bottom. In the case of interest: $p = k$, $q = 2k+1$ the ordering is more complex and depends on the parity of k.

The local behaviour near $k_\parallel = \pi/2$ can be found using second-order degenerate perturbation theory with the following results.

$$\begin{aligned}
&\lambda^0\ (x) \sim 2[2A_k - B_k x^2] && x \to 0 \\
&\lambda^{1-}(x) \sim 2[(A_{k+1} + A_{k+2}) + B_{k+2}x^2] && x \to 0 \\
&\lambda^{1+}(x) \sim 2[(A_{k+1} + A_{k+2}) + (B_{k+2} - 2B_{k+1})x^2] && x \to 0 \\
&\lambda^{i\pm}(x) \sim 2[(A_{k+i} + A_{k+i+1}) + (B_{k+i+1} - B_{k+i})x^2] && x \to 0 \quad i = 2, 3, \ldots, k-1 \\
&\lambda^{k\pm}(x) \sim 2[(A_1 + 1) \pm x + B_1 x^2] && x \to 0
\end{aligned} \tag{5.4}$$

where

$$B_j = \frac{2(A_j)^2}{A_{j-1} - A_{j+1}}$$

and $x = \cos(k_\parallel)$.

This analysis has shed some light on the band structure close to the zone boundary. It is clear that, to second order in x, the eigenvalues are independent of z and hence $k_\perp$ as observed in figure 4. This lack of $k_\perp$ dependence and the fact that there are no $O(x)$ terms leads to peaks in the density of states at the energies $J\lambda^i(0)$ denoted by full circles (●) in figures 6 and 7. The fact that $\lambda^k(x)$ does have a term linear in x is reflected in the fact that there is no peak associated with the energy $J\lambda^k(0)$.

6. Behaviour at the zone centre and the harmonic approximation

The local behaviour of the lowest band at the zone centre is governed by the helicity modulus tensor, $\Gamma_{\mu,\nu}$ where $\mu, \nu \in \{\|, \perp\}$, which is defined by

$$\Gamma_{\mu,\nu} = \left(\frac{\partial^2 \omega^{(0)}(\boldsymbol{k})}{\partial k_\mu \partial k_\nu} \right)_{\boldsymbol{k}=\boldsymbol{0}}. \tag{6.1}$$

This leads to the harmonic approximation

$$\omega^{(0)}(\boldsymbol{k}) \sim \tfrac{1}{2} k_\mu \Gamma_{\mu,\nu} k_\nu \qquad |\boldsymbol{k}| \to 0. \tag{6.2}$$

The helicity moduli are evaluated in [7] with the results

$$\Gamma_{\|,\|} = \frac{4L_+(q)}{q} \qquad \Gamma_{\perp,\perp} = \frac{4q}{L_-(q)} \qquad \Gamma_{\|,\perp} = \Gamma_{\perp,\|} = 0 \tag{6.3}$$

where $L_+(q) = \sum_{i=1}^{q} A_i$ and $L_-(q) = \sum_{i=1}^{q} 1/A_i$. It is notable that the helicity moduli both depend on q only, not on p since different values of p merely permute the A_is. Asymptotically $\Gamma_\| \sim 8/\pi$ and $\Gamma_\perp \sim 2\pi/\ln(q)$ when $q \to \infty$. We can use this approximation to try and estimate the low energy density of states

$$\rho(\omega) = \frac{1}{\pi^2} \int_{-\pi/2}^{\pi/2} \mathrm{d}k_\| \int_{-\pi/2q}^{\pi/2q} \mathrm{d}k_\perp \, \delta(\omega - \omega^{(0)}(\boldsymbol{k})) \qquad \omega < \omega^{(1)}(\boldsymbol{0}). \tag{6.4}$$

Because of the anisotropy of the zone there are two régimes depending on whether ω is less than or greater than $\overline{\omega_q} = \Gamma_\perp \pi^2/8q^2 \sim \pi^3/8q^2 \ln(q)$ with $q \to \infty$. If $\omega < \overline{\omega_q}$ then the contour of contributing states is a closed ellipsoid (cf figure 3) and the fluctuations are two-dimensional in character, if $\omega > \overline{\omega_q}$ then the ellipsoid is truncated by the zone boundary at $k_\perp = \pm\pi/2q$ and the behaviour starts to look more one-dimensional as seen in the exact results of section 4. Substituting the expression (6.2) into (6.4) and re-arranging gives

$$\rho(\omega) = \frac{2}{\pi^2 \sqrt{\Gamma_\| \Gamma_\perp}} \int_0^{\min\{\omega, \overline{\omega_q}\}} \frac{\mathrm{d}u}{\sqrt{\omega u - u^2}} \tag{6.5}$$

which yields

$$\rho(\omega) = \frac{2}{\pi \sqrt{\Gamma_\| \Gamma_\perp}} \left\{ \theta(\overline{\omega_q} - \omega) + \theta(\omega - \overline{\omega_q}) \left[\frac{1}{2} - \frac{1}{\pi} \sin^{-1}\left(1 - \frac{2\overline{\omega_q}}{\omega} \right) \right] \right\}. \tag{6.6}$$

For large ω this has the asymptotic form

$$\lim_{\omega \to \infty} \rho(\omega) = \frac{2}{\pi^2 \sqrt{\Gamma_\| \Gamma_\perp}} \sqrt{\frac{2\overline{\omega_q}}{\omega}}.$$

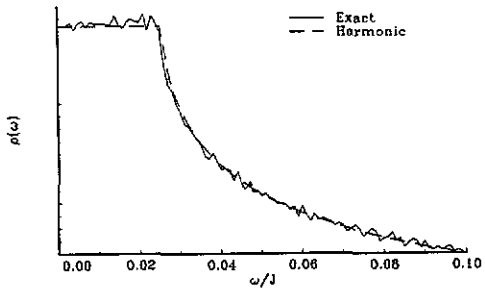

Figure 8. The low energy density of states for $f = 4/9$: full curve, exact numerical result; broken curve, harmonic approximation

The harmonic approximation for f=4/9, where $\overline{\omega_9} \approx 0.02J$, is shown in figure 8 in comparison with the exact low energy density of states.

This approximation is of course only valid for $\omega < \omega^{(1)}(0,0)$. We can find an upper bound on this, the bottom of the next band up, as follows. The zero mode corresponding to $\omega^{(0)}(\mathbf{0})$ is $C_j = 1/\sqrt{q}$, we therefore use the trial state $C_j = (1/\sqrt{q})e^{ij\pi/q}$, which is exact for $f = 0$: taking the expectation value of the reduced Hessian, **H** of (5.1), at the zone centre in this state gives an upper bound on the bottom of the first band up

$$\omega^{(1)}(\mathbf{0}) \leqslant C^{\dagger}\mathbf{H}C = 4\sum_{j=1}^{q} A_j(1 - \cos(\pi/q)) = 8\sin\left(\frac{\pi}{2q}\right). \tag{6.7}$$

For large q this gives $\omega^{(1)} \leqslant 4\pi/q$.

This behaviour is not confined to the lowest band, it occurs for all of them, which explains the remaining peaks in the densities of states of figures 6 and 7 which are marked by + signs.

7. Discussion

It has been shown that the fluctuation spectra of the frustrated XY model around the flux density wave states are rather complicated with many peaks associated with the fact that the bands are very flat in the $k_\perp$ direction and that many constant energy surfaces are cut by the long zone boundary leading to quasi-one-dimensional behaviour: the peaks can thus be thought of as van Hove singularities which are cut off by the small 2D-like regions close to the band extrema. It is to be hoped that at least some of these features may be observable in artificial superconducting arrays, for example in microwave absorption experiments. The limit $k \to \infty$ for fixed L of the sequences studied clearly represents an incommensurate system (the sequence $f_k = p_k/q_k : p_k = q_{k-2}, q_k = q_{k-1} + q_{k-2}$ which generates successive rational approximants to the irrational number $1 - g$, where g is the golden mean $g = 1/(1 + g)$, would be of more interest in this case) but it is not at all clear that for q larger than a certain value the flux density wave is the ground state and it is even less clear that the fluctuation analysis presented above has any meaning since for a true incommensurate system $q > L$ and there are no points sampled off the $k_\perp$ axis.

Acknowledgments

I am most grateful to M A Moore for introducing me to this subject and for many helpful discussions. This work was supported by the SERC. The numerical diagonalization was performed using NAG library routines.

References

[1] Teitel S and Jayaprakash C 1983 *Phys. Rev. Lett.* **51** 1999
[2] Teitel S and Jayaprakash C 1983 *Phys. Rev.* B **27** 598
[3] Shih W Y, Ebner C and Stroud D 1984 *Phys. Rev.* B **30** 134
[4] Müller K A, Takashige M and Bednorz J G 1987 *Phys. Rev. Lett.* **58** 1143
[5] Rosenblatt J, Pegral P, Raboutrou A and Lebeau C 1988 *Physica* B **152** 95
[6] Hofstadter D R 1976 *Phys. Rev.* B **14** 2239
[7] Halsey T C 1985 *Phys. Rev.* B **31** 5728
[8] Halsey T C 1985 *J. Phys. C: Solid State Phys.* **18** 2437
[9] Choi M Y and Doniach S 1985 *Phys. Rev.* B **31** 4516
[10] Choi M Y and Stroud D 1985 *Phys. Rev.* B **32** 7173
[11] Korshunov S E and Uimin G V 1986 *J. Stat. Phys.* **43** 1
[12] Benedict K A and Moore M A 1989 *Phys. Rev.* **39** 4592
[13] Kardar M 1986 *Phys. Rev.* B **33** 3125
[14] Benedict K A 1989 *J. Phys.: Condens. Matter* **1** 4895
[15] Benedict K A 1990 *J. Phys. A: Math. Gen.* **24** 689
[16] Lobb C J 1989 *Physica* B **152** 1
[17] Wilkinson M 1984 *J. Phys. A: Math. Gen.* **17** 3459